iScience

CellPress
OPEN ACCESS

Article

The use of novel electronic nose technology to locate missing persons for criminal investigations

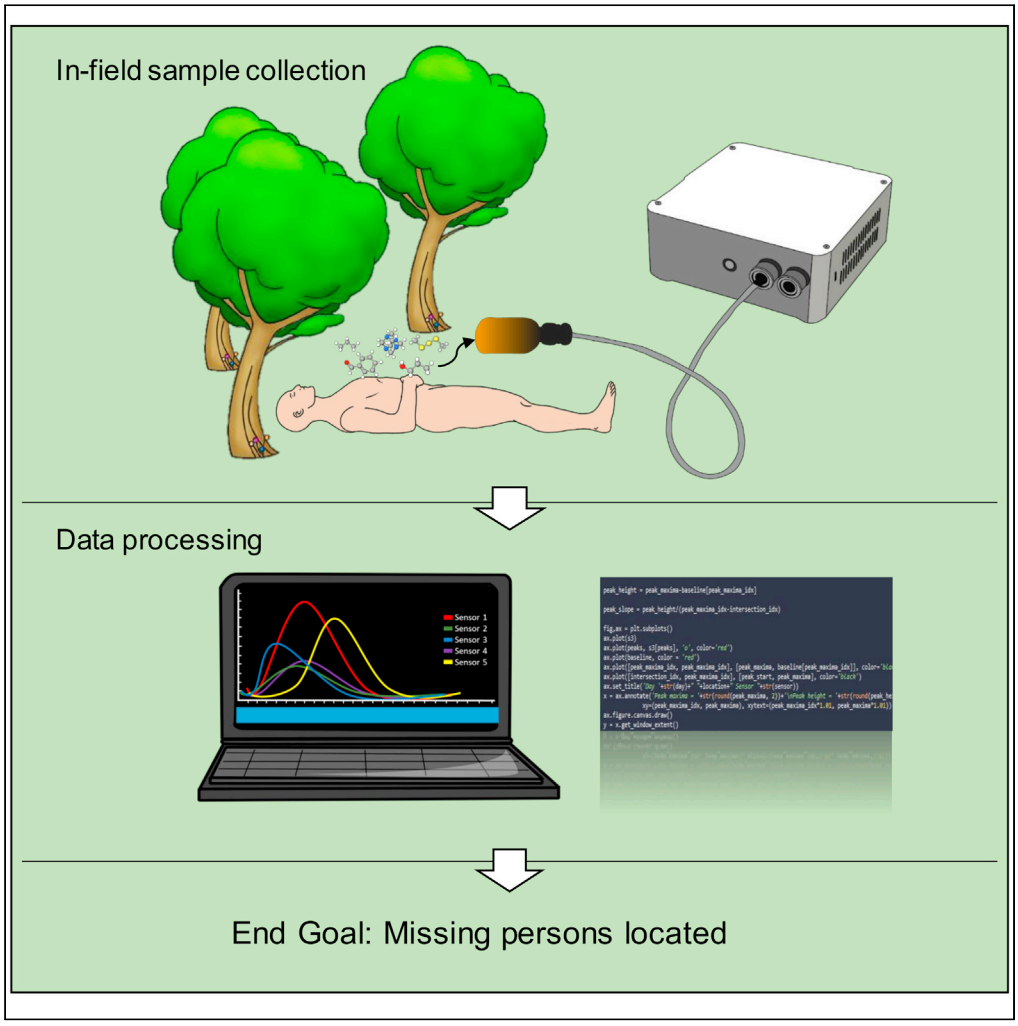

Amber Brown, Erin Lamb, Alisha Deo, ..., Wentian Zhang, Steven Su, Maiken Ueland

maiken.ueland@uts.edu.au

Highlights

Electronic Nose was able to detect human-decomposition VOCs in outdoor environment

Sensor responses supported through VOCs detected by GC×GC-TOFMS

Sensors were influenced by change in temperature, wind direction, and gust speed

Distinct sensor responses recorded due to differential decomposition

Brown et al., iScience *26*, 106353
April 21, 2023 © 2023 The Author(s).
https://doi.org/10.1016/j.isci.2023.106353

iScience

CellPress
OPEN ACCESS

Article

The use of novel electronic nose technology to locate missing persons for criminal investigations

Amber Brown,[1,2] Erin Lamb,[1] Alisha Deo,[1] Daniel Pasin,[1] Taoping Liu,[3] Wentian Zhang,[3] Steven Su,[3,4] and Maiken Ueland[1,5,*]

SUMMARY

The search for missing persons is a major challenge for investigations involving presumed deceased individuals. Currently, the most effective tool is the use of cadaver-detection dogs; however, they are limited by their cost, limited operation times, and lack of granular information reported to the handler. Thus, there is a need for discrete, real-time detection methods that provide searchers explicit information as to whether human-decomposition volatiles are present. A novel e-nose (NOS.E) developed in-house was investigated as a tool to detect a surface-deposited individual over time. The NOS.E was able to detect the victim throughout most stages of decomposition and was influenced by wind parameters. The sensor responses from different chemical classes were compared to chemical class abundance confirmed by two-dimensional gas chromatography – time-of-flight mass spectrometry. The NOS.E demonstrated its ability to detect surface-deposited individuals days and weeks since death, demonstrating its utility as a detection tool.

INTRODUCTION

The location and recovery of human remains is critical for forensic (homicide, suicide, missing persons) and mass disaster investigations. Over 30,000 people are reported missing each year in Australia alone.[1,2] In Australia, if missing persons are not located after three months, they are then categorized as "long-term missing persons".[1] At this point, the investigations may shift focus from the location of a living victim to the recovery of human remains. Alternatively, if foul play is suspected, the search efforts to locate the presumed deceased individual may begin immediately once the person is reported missing. The prompt discovery of human remains is critical for forensic investigations, including the rapid physical identification of individuals, the collection of biological evidence, and the establishment of an approximate time since death. Regardless of timeline, the discovery of missing and presumed deceased individuals is one of the most intractable challenges to date in criminal investigations.[3]

Several detection methods are currently available for the discovery of deceased victims. These methods include visual search efforts by human search teams,[4–7] the use of remote-imaging techniques,[8–10] and the implementation of cadaver-detection dogs.[11] The success of physical ground searches conducted by search teams relies on visual clues, including physical changes to the immediate surrounding environment, such as disturbed or changed vegetation or soil.[4,5,12–14] The number of personnel available, weather conditions, and physical limitations such as fatigue limit human-based search efforts. Additional search methods rely on specialized technology such as geophysical technology (ground-penetrating radar [GPR][15,16]) or aerial surveillance (light detection and ranging [LiDAR] and digital photometry[8–10]) to locate deceased individuals. A variety of environmental factors can impact the field use of these specialized technologies. For example, the reliability of GPR can be impacted by anomalies (dense rock, tree roots or objects, or burst water pipe)[17] and is unable to be deployed in bodies of water or areas of rocky terrain.[18,19] However, the success of each of these search efforts is impacted by time of day, weather conditions, and type of terrain.[7,20]

The most efficient tool for victim discovery is the use of cadaver-detection dogs. These dogs are specifically trained to detect the volatile organic compounds (VOCs) that are released from deceased and decomposing individuals. As a deceased individual undergoes decomposition, VOCs are created through the catabolism of the major biological macromolecules (proteins, carbohydrates, and lipids).[21–25] These VOCs are

[1]Centre for Forensic Sciences, School of Mathematical and Physical Sciences, University of Technology Sydney, Sydney, NSW 2007, Australia

[2]Australian Museum Research Institute, Australian Museum, Sydney, NSW 2001, Australia

[3]Faculty of Engineering and Information Technology, University of Technology Sydney, Sydney, NSW 2007, Australia

[4]College of Artificial Intelligence and Big Data for Medical Science, Shandong First Medical University & Shandong Academy of Medical Sciences, Jinan 250117, China

[5]Lead contact

*Correspondence: maiken.ueland@uts.edu.au

https://doi.org/10.1016/j.isci.2023.106353

This is an open access article under the CC BY-NC-ND license (http://creativecommons.org/licenses/by-nc-nd/4.0/).

constantly produced throughout all stages of decomposition[22] and diffuse into the surrounding environment. The dispersal of VOCs from decomposing human remains allows for their detection by these specialized detection dogs.

Despite their profound detection abilities, the use of cadaver-detection dogs can be augmented through the use of portable electronic detection technology. These canines are expensive to train and maintain, are prone to handler bias, may alert to false positives (alerting to deceased, non-human animals), and are limited in working hours.[26,27] The use of electronic technology may provide real-time and explicit feedback of what chemical odors are being tracked allowing handlers to determine whether dogs are detecting decomposing human remains or other closely related conspecifics. VOCs produced by human remains have been investigated for decades[21,24,28–31] and are generally established; this allows for the targeting of selected potential biomarkers for detection purposes.

Instrument-based approaches for the collection and identification of VOCs produced by decomposing human remains currently rely on a two-step process whereby samples are collected in field and analyzed using benchtop instrumentation (chromatography coupled with mass spectrometry [GC-MS][32] and comprehensive two-dimensional gas chromatography coupled with time-of-flight mass spectrometry [GC×GC-TOFMS]).[22,28] Though accurate, these methods are not portable and expensive, which limits their applicability in the real-time detection of human remains. To address this gap, portable technology-based solutions, such as electronic noses (e-noses) are a potential alternative to expensive benchtop equipment for the detection of VOCs. E-noses are portable, or semi-portable, instruments that mimic mammalian olfaction through the use of multi-sensor arrays.[33] E-nose systems generally consist of one sampling and one reference gas inlet, multi-sensor arrays, an information-processing unit, and software that uses pattern-recognition algorithms.[33] This configuration allows the detection and identification of differences in the components present in the vapor mixture. To date, e-noses have been applied to a wide range of detection applications ranging from the identification of spoiled foods, the detection of hazardous industrial and environmental pollutants, and the detection of volatile biomarkers for diagnostic applications.[33–36] However, this technology has not yet been applied for the detection of decomposing human remains.

In order for e-nose technology to be effective in an outdoor environment for the detection of human remains, the principles of scent detection must be considered. Firstly, as VOC production changes throughout the decomposition process, the presence of certain human decomposition-specific VOC chemical classes must be considered. For example, during the active stages of decomposition, both the classes and abundances of VOCs are produced at a higher rate than during the earlier and later stages of decomposition. Due to the disparity of VOC presence and abundance produced across decomposition stages, appropriate sensors must be selected to encompass these changes in order for e-noses to be adapted for the detection of human remains. The second principle relies on the detection of VOCs as they are diluted into the environment. E-nose sampling devices should be designed to capture VOCs of differing volatilities and dispersal mechanisms following the release by decomposing human remains. Generally, VOC diffusion from human remains follows that of other odourous targets, by which scents are dispersed through a ''scent cone''. Specifically, this refers to the diffusion of VOCs from the areas of highest concentration (near the body) to areas of lower concentration in the surrounding environment.[37] To locate the target, it is most effective to locate the outer edges of the scent cone and work within to locate the source.[11] The size and shape of the scent cone can be affected by multiple factors, including environmental (terrain) and weather (humidity, temperature, wind dispersion) factors.[11] It is then relevant to compare e-nose responses in relation to differing environmental and climatic conditions to assess the impact of these factors on detection ability. This assessment will aid in determining whether this instrument can be used to detect a dispersing scent cone, as well as its cross reactivity to other environmental factors.

This work presents the very first use of e-nose technology for the detection of VOCs produced by decomposing human remains in different decomposition stages in an outdoor environment. This work utilized an e-nose (NOS.E) developed as a collaboration between the University of Technology (UTS) Center for Forensic Science and the UTS School for Biomedical Engineering[38] equipped with five metal-oxide (MOX) gas sensors. The averaged maximum sensor responses recorded by the e-nose when sampling human-deposited human remains were compared to environmental controls and environmental parameters (average daily temperature, gust speed, and wind direction). In addition, NOS.E sensor responses were compared to analytical results produced by GC×GC-TOFMS as this method is the current gold

standard for identifying VOCs produced by human decomposition.[28,29,31,39] This analysis was conducted to determine whether the NOS.E was reacting to VOCs related to human decomposition or was cross-reacting with environmental VOCs of the same chemical class.

RESULTS

Environmental data

The average temperature throughout the period of study was 15.3°C (Figure S1), with the average daily temperature decreasing steadily during the trial (~19–20°C to 9–12°C). A total rainfall of 37.6 mm was recorded but occurred sporadically throughout the study. Four main periods of rain were observed, from day of placement until day 5, between days 8–9, and two major spikes between days 35–36 and 57–63 post-placement. The site experienced an average relative humidity of 79% over the course of the study. Wind speed was recorded as being negligible as the average wind speed over the study was not high enough to impact the NOS.E.

Cadaver decomposition visual observations

Visual decomposition was classed using the stages of decomposition as defined by Payne, King[40] to investigate the rates of decomposition experienced by the two different sampling regions for the NOS.E. The two investigated areas (head and torso) were found to decompose at different rates (Figure S2).

The head decomposed at a faster rate than the torso, with the head entering the bloat stage on day 4. The torso began to feature bloat characteristics by day 10, followed by the limbs on day 13. By this time, the head had entered into active decay followed by advanced decay by day 18. Large amounts of discoloration were observed across the body during active decay, and the donor (apart from the head) was in active decay on day 16. The skin of the torso blackened and hardened toward day 40, which alongside excessive amount of mass loss indicated that the donor had entered advanced decay. The skull of the donor was visible by this stage, indicating that the head had entered the final decomposition stage. The torso remained in advanced decay for the remainder of the sampling period, with little visual changes observed.

Initial NOS.E results

Initially, NOS.E sampling of the donor was only conducted over the torso region as it was suspected that this region would be the center of the scent cone. However, by day 5, pronounced differential decomposition was observed, and samples were taken from both the head and torso region from this day onwards. For a visual comparison of sensor responses across sampling areas, a heatmap was generated representing the averaged maximum sensor responses across replicates (n = 5) per region per sampling day (Figure 1). Maximum sensor responses were recorded during active decay for both the head and torso region (day 7 and day 16, respectively). Overall, it was found that the torso had a lower average signal response from all responding sensors as compared to the head. The data showed that the sensors responded to decomposition-like VOCs during the sampling of the control environment, particularly on day 41 and 59. The effect of environmental conditions on the NOS.E responses was further investigated.

Impacts of environmental parameters and decomposition to NOS.E responses - Head sampling

The sampling of the head region began on day 5 (Figure 2) due to a clear visual difference in decomposition between the head region and the remainder of the body on this day. All sensors (apart from sensor 3) responded to the fresh, bloat, and active decay stages during the first 16 days of placement. From day 41 onwards, there were limited sensor responses to the head region. A decrease in sensor responses was seen on day 10, relative to day 7 and 13 (Figure 2). Increased wind gust speeds were present on day 10 (Figure 2B); however, there were limited changes in temperature and wind direction in this period (Figures 2A and 2C). The lowest sensor responses (Day 41 and 59) of the NOS.E from the head region were associated with the change in wind direction from East (E)/ North East (NE) to West (W)/North West (NW) (Figure 2C) and a decrease in temperature (Figure 2A).

Impacts of environmental parameters and decomposition to NOS.E responses - Torso sampling

There were limited sensor responses from the torso until day 5 postmortem (Figure 3). From day 7, sensors 1 and 2 (alcohol and alkanes) responses increased until reaching a maximum on day 13 (Figure 3).

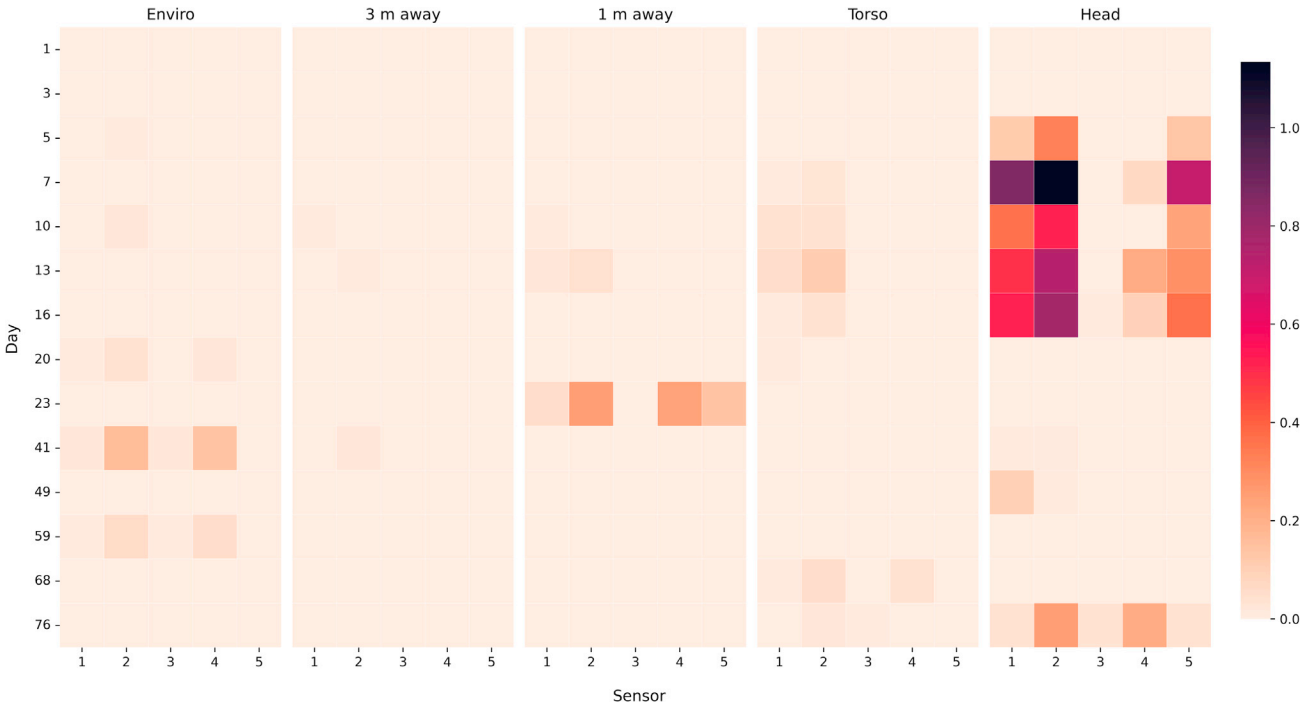

Figure 1. Heatmap of sensor responses

Heatmap created from the averages of each sampling region and sampling day, with both human regions, 3 m away, 1 m away and the environmental control (Enviro) included.

This increase was consistent with the torso progressing from the bloat stage toward the active decay stage.

A decrease in sensors 1 and 2 responses were observed on day 16 and 20. As with the head sampling, torso sampling was also affected by environmental conditions. Specifically, the highest average sensor responses were recorded at lower wind gust speeds (Figure 3B) and when winds were blowing E/NE (Figure 3C). There appeared to be no correlation between the change in average maximum sensor response and temperature, apart from the later sampling days (Figure 3A). Prior to sampling days 68 and 76, alcohols/alkanes were not detected. The sensor responding to alkanes alone (sensor 3) did not react above the baseline threshold during the course of the trial, apart from on day 76. Following a period of no sensor responses, on day 68, sensors 1, 2, and 4, all responded to the torso region. These recordings were made

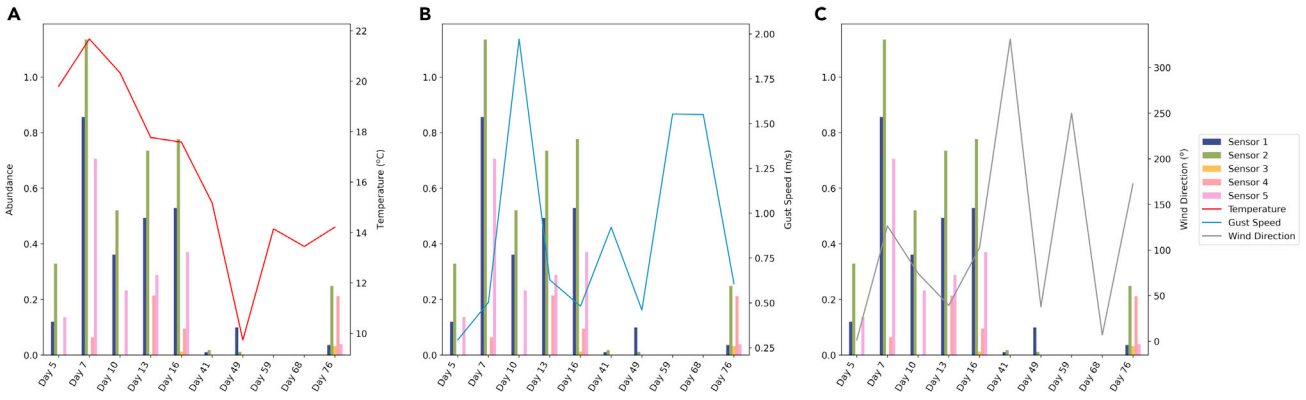

Figure 2. NOS.E sensor responses

Sensor responses for the head sampling region with environmental parameters: A. temperature, B. wind gust speed, and C. wind direction.

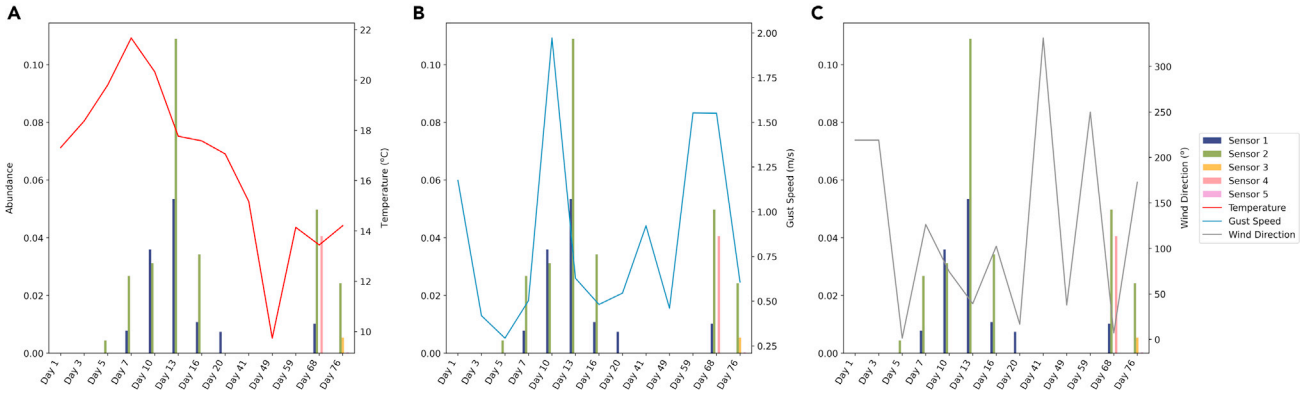

Figure 3. NOS.E sensor responses

Sensor responses for the torso sampling region with environmental parameters: A. temperature, B. wind gust speed, and C. wind direction.

after a period of heavy rainfall (12 mm, Figure S1), over a third of the total rainfall for the trial period. This day was also the first time a sensor reactive to sulfur/nitrogen responded in this region.

Impacts of environmental parameters and decomposition to NOS.E responses - 1 m and 3 m sampling

The results were limited with average maximum sensor responses above baseline occurring on days 10, 13, and 23 and days 10, 13, and 41 for the 1 and 3 m away sampling areas, respectively (Figures 4A–4F). More relevant to the change of average maximum sensor response was the change in temperature and wind direction from E/NE to South (S)/South East (SE) (Figure 4C) for 1 m away and from E/NE to West (W)/North West (NW) for 3 m away (Figure 4F).

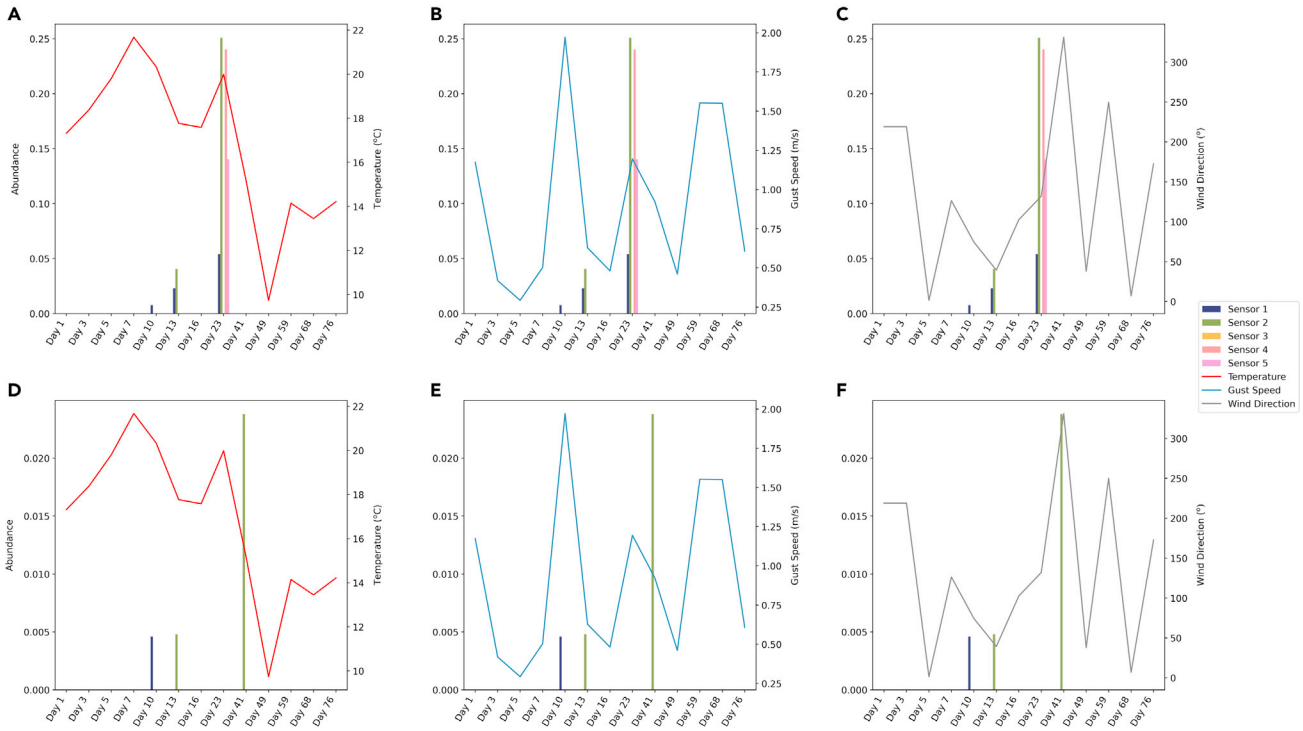

Figure 4. NOS.E sensor responses

Sensor responses for the 1 m sampling region with environmental parameters: A. temperature, B. wind gust speed, and C. wind direction. NOS.E sensor responses for the 3 m sampling region with environmental parameters: D. temperature, E. wind gust speed, and F. wind direction.

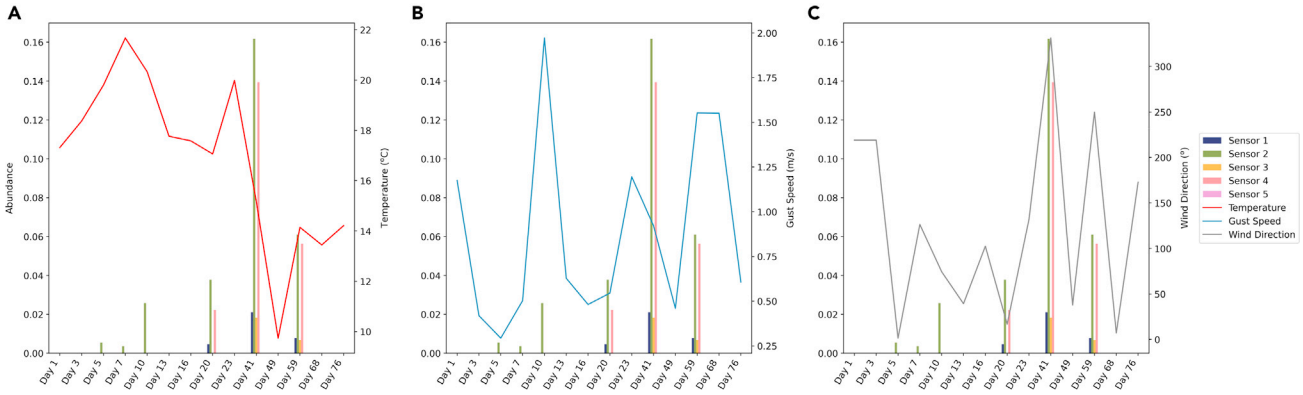

Figure 5. NOS.E sensor responses

Sensor responses for the environmental sampling region with environmental parameters: A. temperature, B. wind gust speed, and C. wind direction.

Impacts of environmental parameters and decomposition to NOS.E responses - Environmental sampling

The scale of the sensor response was much lower for environmental replicates and was not detected on every sampling day (Figure 5). The maximum responses from environmental controls occurred when the winds shifted from the W/NW to the W/South West (SW) (Figure 5C).

Principal-component analysis (PCA)

From the visual observation of the PCA, the NOS.E produced similar sensor responses from 1 m away during the fresh, bloat stage and advanced decomposition stage (Figure 6B). A change in the sensor responses was determined during the active decomposition stage from this region. There was little difference seen in NOS.E detection and decomposition state when located from 3 m away (Figure 6A) or over the torso (Figure 6C). The NOS.E was, however, able to distinguish all recorded decomposition stages from the head region (Figure 6D). The most pronounced difference was between the advanced and active decomposition stages.

GC×GC-TOFMS results

To determine the ability of the NOS.E to detect VOCs associated with human decomposition, the sensor response results were compared to GC×GC-TOFMS analysis (an example contour plot can be seen in Figure S3). Initially, the abundances of the full dataset (all functional groups) were analyzed to get a better understanding of the overall volatilome emitted from the cadaver (Figure 7). The VOC profile was found to be changing over time with an increase in the VOC abundance during days 14 and 16, corresponding to the bloat and active decay stage overall. The data shows a large presence of alcohols and sulfides, both compound classes detected by the NOS.E.

In order to further compare the GC×GC-TOFMS data directly to the NOS.E sensor responses, selected compound classes were investigated further (Figure 8). These classes were selected as they correspond to those compound classes detected by the NOS.E.

Alcohols were found to be the major contributing class in the VOC analysis and exhibited a clear increasing trend until day 14, before decreasing steadily until the end of the trial. Alkanes fluctuated over the course of decomposition but generally exhibited an increase over time until day 40. The relative abundance of sulfides trended similarly to the abundance of alcohols. Sulfide (S)-containing compounds were not present in large abundances in the mid to later stages of decomposition (active and advanced). Nitrogen (N)-containing compounds had a more defined trend in the GC×GC-TOFMS analysis, by which the relative abundance increased until day 7, before decreasing until they were no longer detected on day 60.

DISCUSSION

A human donor was placed in an outdoor scenario, and volatile samples were taken using electronic nose technology from several regions above and away from the donor. Samples were also collected using GC×

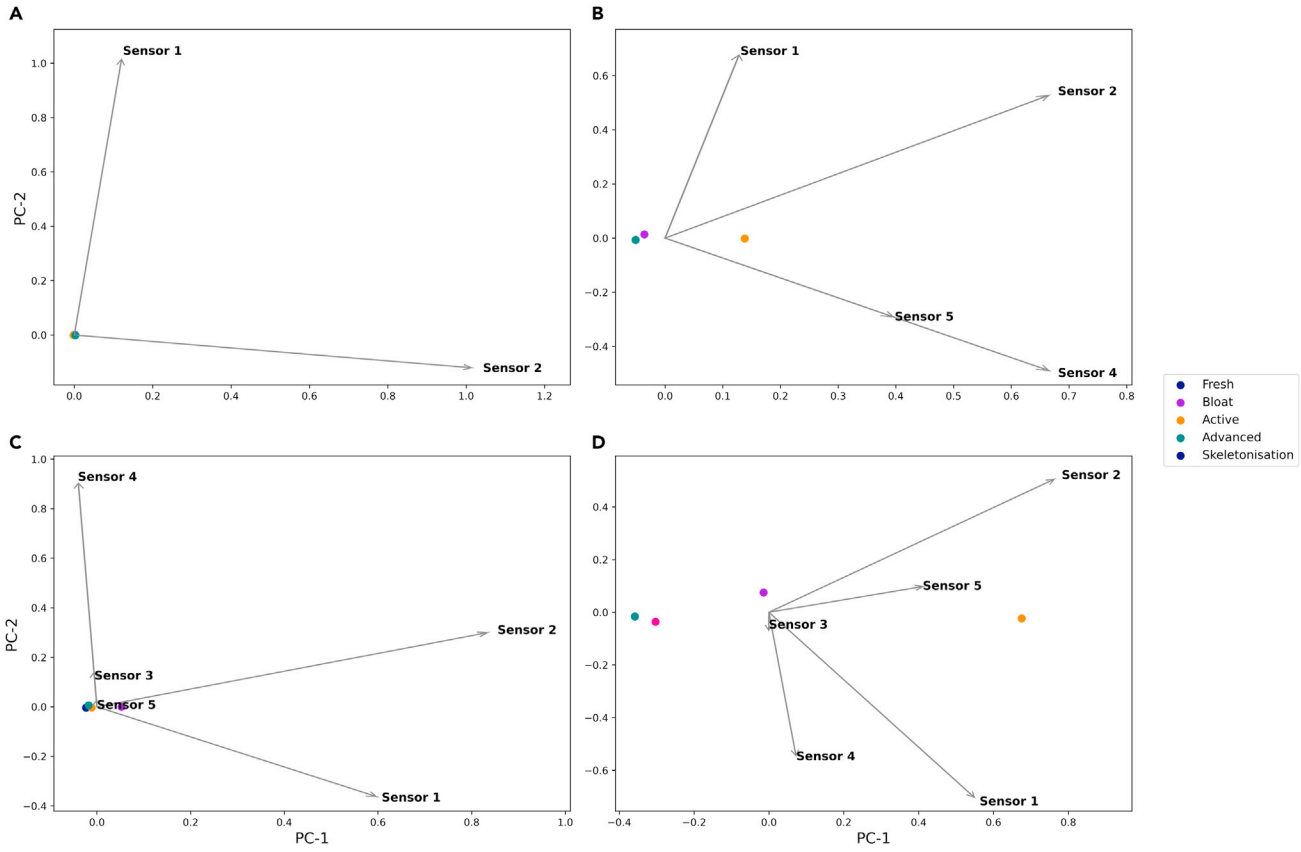

Figure 6. Principal-component analysis of the NOS.E sensor

NOS.E sensor responses grouped according to the visual decomposition stages for A. 3 m away, B. 1 m away, C. Torso, and D. Head regions.

GC-TOFMS, the current gold standard for VOC analysis, for comparison and confirmation. The study was conducted in the Australian autumn season going into winter when temperatures are low. The slow progression of decomposition that was determined visually with the human donor is consistent with other research whereby decomposition (and subsequent VOC production) is known to be much slower in the colder seasons than during warmer temperatures.[23,28,31,41] These results also revealed an extreme amount of differential decomposition, which is supported by the literature.[29,42] This differential decomposition likely affected the abundance and classes of VOCs being emitted from each region. Despite the colder environment and reduced VOC production, the NOS.E was able to record sensor signals throughout the trial, demonstrating its potential as a detection tool.

Sensor responses

Overall it was shown that the head region had the most pronounced sensor responses. The increased sensor response of the head region may be attributed to the faster decomposition rate (Figure 2) coupled with the limited surface area that may have pre-concentrated the decomposition VOCs in this area. Conversely, the slower decomposing and large surface area associated with the torso region may have reduced the VOC detection. This finding will likely impact the dispersal of the scent cone as well as which sensors are demonstrating the most specific signals related to decomposition VOCs.

There were some sensor responses when sampling the control environment. These responses are likely due to the environmental factors, such as wind conditions and temperature, documented during the days these sensor responses were seen. Environmental factors may have impacted the sensor responses to the controls as the sampling occurred within the bounds of Australian Facility for Taphonomic Experimental Research (AFTER) where multiple cadavers are present in differing stages of decomposition. Attempts were made to ensure that no cross-contamination occurred by taking the control samples at a far distance

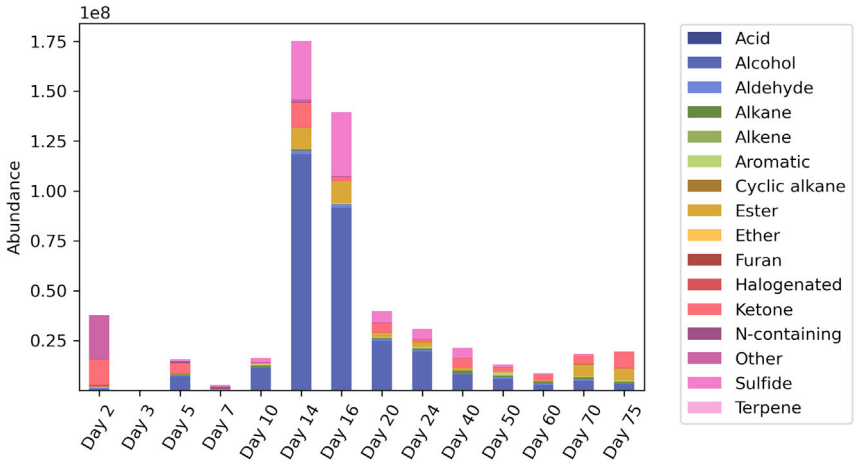

Figure 7. Complete GC×GC-TOFMS VOC profiles of the decomposing human over the course of the study

from any other donor (over 100 m). However it is likely that the control sensor responses recorded were not influenced by the specific cadaver used for this study, but instead were impacted by the higher abundance of decomposition VOCs from multiple cadavers at the site. Future work should collect the control samples even further away and determine wind direction prior to sampling.

Region-specific sensor responses – Head

The head region sampling commenced on day 5 due to the degree of differential decomposition observed. During the first 16 days post-placement, majority of the sensors responded to the human donor and could be used for the detection of the victim. From day 7 to day 13, large sensor responses were observed and mimicked the literature as this corresponded to the active decay stage, the stage known to be the most odorous.[22,43,44] Once the head region was at the end of advanced decay stage, and transitioned to skeletonization, limited sensor responses were detected. This period is associated with reduced levels of VOC production.[23]

A decrease in sensor responses was seen on day 10, relative to day 7 and 13 (Figure 2). This is likely associated with the increased wind gust speeds on day 10 (Figure 2B) as there were limited changes in temperature and wind direction in this period (Figures 2A and 2C). Generally, the NOS.E had the highest sensor responses over the head region when the wind gust speeds were the lowest (Figure 2B) during active decomposition. The lowest sensor responses (day 41 and 59) of the NOS.E from the head region were associated with the change in wind direction from E/NE to W/NW (Figure 2C) and a decrease in temperature (Figure 2A). The change in wind direction was hypothesized to impact the NOS.E response as the signal increased on the final sampling day when the wind direction returned to E/NE, even on the coldest sampling day (day 49; Figures 2B and 2C) when the head was in the skeletal stage.

Region-specific sensor responses – Torso

There were limited sensor responses from the torso until day 5 postmortem (Figure 3). Very few VOCs are reported during the early stages of decomposition due to limited amounts of bacterial and microbial activity.[23] These findings were therefore consistent with the literature, particularly as the study was conducted during colder temperatures, known to reduce VOC emittance.[28,41,43]

From day 7, sensors 1 and 2 (alcohol and alkanes) responses increased until reaching a maximum on day 13 (Figure 3). This increase was consistent with the torso progressing from the bloat stage toward the active decay stage. Increases in VOC abundances are most commonly reported during the active decay stage, before decreasing with the disappearance of soft tissue during advanced decay.[21–24,41,45] The largest sensor responses were measured during the bloat stage and not the active decay stage, which was unexpected. This is suspected to be due to the differential decomposition observed and the close proximity of the head and other regions, which exhibited more advanced decomposition than the torso.

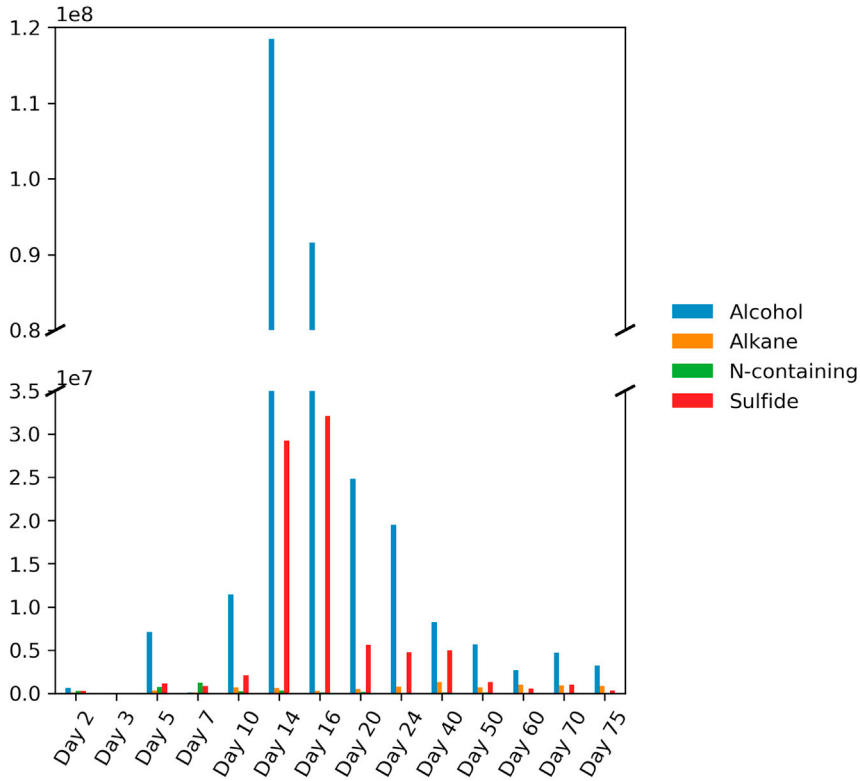

Figure 8. Selected chemical classes detected from the decomposing remains using GC×GC-TOFMS

A decrease in sensors 1 and 2 was observed on day 16 and 20. As with the head sampling, torso sampling was affected by environmental conditions. Specifically, the highest average sensor responses were recorded at lower wind gust speeds (Figure 3B) and when winds were blowing E/NE (Figure 3C). Although the NOS.E responded to the different decomposition stages and the environment, the change in average maximum sensor response did not appear to be correlated with a temperature change, except on later days, 68 and 76 (Figure 3A). Prior to these days, alcohols/alkanes were not detected. Alcohols and alkanes are commonly seen early in the decomposition process particularly the fresh and bloat stages of decomposition.[22,23,29] The sensor responding to alkanes alone (sensor 3) did not react above the baseline threshold, apart from on day 76. Therefore, it could be construed that the sensors 1 and 2 (targeting alcohols and alkane compounds) were most likely responding to alcohol VOCs. Alcohols are commonly observed in the middle stages of decomposition and results from bacterial degradation and fermentation of fatty acids and carbohydrates.[23,46] Following a period of no sensor responses, on day 68, sensors 1, 2, and 4 all responded to the torso region. These recordings were made after a period of heavy rainfall (12 mm, Figure S1), over a third of the total rainfall for the trial period. The rainfall was therefore suspected to have rehydrated the body, allowing for more decomposition to occur and thus the release of VOCs.

Sensor responses away from the donor

There were limited sensor responses for the 1 and 3 m distances away from the donor. Signal was noted to be influenced by the wind direction and temperature, specifically E/NE to S/SE wind direction (Figure 4C) for 1 m away and from E/NE to W/NW wind direction for 3 m away (Figure 4F). The increased dispersal of the scent cone may be attributed to the increase of the ambient temperature as well as the changing wind direction. As samples were taken in the same location during each sampling period, and not in relation to wind direction, it is likely that the NOS.E sampling position affected the detection of decomposition VOCs.

The scale of the sensor responses from the environmental area was much lower (Figure 5). The maximum responses were again influenced by the wind direction, particularly when the winds shifted from the W/NW

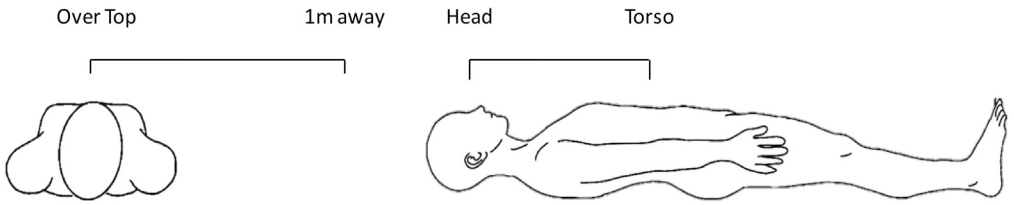

Figure 9. Sampling locations for the NOS.E

All sampling locations used in the trial, including torso, head, 1 m away, and 3 m away. The environmental control located 100 m upwind is not shown.

to the W/SW (Figure 5C). Due to the location of the current study within the AFTER facility, all other surface donors (>50) were located SW of the sampled cadaver, the closest of which was over 30 m away. Thus, there is the potential that the increased sensor response on those days may be attributed to other decomposing donors on the property. Due to the response from the environmental controls, future research should conduct environmental sampling in areas where there are no human cadavers within a much larger radius.

Time since death estimation potential

Changes in sensor responses over time from each location could be visualized. In terms of the samples taken at 1 m away from the donor, it was determined that the sensor responses between the fresh, bloat stage and advanced decomposition stage were comparable. The active stage on the other hand was distinct, due to sensors 2, 4, and 5. If applied in a field scenario, it is recommended for the investigator to focus on signal response changes of the sensors mentioned above in order to locate human remains.

PCA revealed little changes in sensor responses over time from the torso and 3 m away. This may be due to environmental dispersal mechanisms that may have diluted the human decomposition VOCs, or due to the stationary placement of the NOS.E during sampling that would have prevented the detection of the scent cone when wind direction changed. Future work should include more active, moving sampling with the NOS.E in order to locate the dispersing scent cone produced by human remains. From a detection perspective, it is not concerning that the NOS.E did not distinguish decomposition stages from the samples taken above the torso. The goal of the detection tool is to locate the remains; therefore, the key is to determine the sensor responses that lead investigators to the body. Additional methods such as visual stages and entomology can then be employed to determine time since death.

There was one region that demonstrated time-dependent sensor responses; the head region. The differing results from the head region were attributed to the differential decomposition observed for this region. For this area a pronounced difference was observed between the advanced and active decomposition stages (Figure 6D). This is concurrent with the literature as most chemical changes resulting from the decomposition process occur during the bloat and active stages.[47,48] The change in sensor responses over the course of decomposition in the head regions is encouraging and demonstrated that this tool has the potential to both locate and assist with the Postmortem interval (PMI) estimation. However, future work is required to improve the sensor responses in all regions to better trap and concentrate the VOCs.

GC×GC-TOFMS analysis

The sensor responses of the NOS.E cannot be directly compared to other analytical equipment, due to the differing approaches. However, some comparisons were made through the identification of compounds by GC×GC-TOFMS. For the most part, the e-nose sensor responses from alcohol, alkenes, and S-containing compounds mimicked trends recorded by the GC×GC-TOFMS data taken from the headspace over the surface remains. This indicates that the sensor responses are more specifically tailored to the decomposing human remains as opposed to other environmental VOCs that may be cross-reactive to the sensors.

Contrary to the NOS.E data, the VOC sampling for the GC×GC-TOFMS analysis was conducted in an environmentally controlled setting by which the whole cadaver was enclosed under an aluminum hood. It is therefore expected that the degree of differential decomposition observed will influence the whole VOC profile, rather than being area specific. The collection method also differs as it involves the accumulation of gases for 15 min prior to sampling, which will pre-concentrate the VOCs in the headspace. Despite

these differences, the comparisons were conducted to identify if the chemical classes being detected by the NOS.E were being produced by the cadaver.

Alcohols were found to be the major contributing class in the VOC analysis and exhibited a clear increasing trend until day 14, before decreasing steadily until the end of the trial. A similar trend was observed by Dubois et al.[49] when analyzing the volatiles released from various tissue samples. The GC×GC-TOFMS data support the findings by the NOS.E as sensors 1 and 2, detecting alcohols and alkanes were responding on most days beyond day 5. The large relative abundance of alcohols detected by the benchtop instrument on days 14 and 16 also corresponds to the increased sensor responses by the NOS.E samples for both the head and torso regions.

Alkanes fluctuated over the course of decomposition but generally exhibited an increase over time until day 40. This may be due to the chemical nature of alkanes as they are generally a less reactive class of compounds compared to the other targeted classes. The fluctuation in compound retrieval by the sorbent material (during VOC analysis) and reaction to the MOX sensors (for the NOS.E) could have been dependent on which specific alkane compounds were present or the changing biological nature of decomposition. A direct comparison of the relative abundance of chemical classes detected by GC×GC-TOFMS to the NOS.E responses is challenging due to the different sampling conditions, dispersal rates of VOCs, and due to the fact that the NOS.E sensors have a collective response to both chemical classes (alcohol and alkanes). The average maximum response of the NOS.E sensors was the highest to the alcohol/alkane sensors (Figure 2 and 3), which was supported by relative compound abundance detected by GC×GC-TOFMS (Figure 8). However, it is likely that a majority of this maximum response can be attributed to alcohols as the alkane-specific sensor did not respond on a majority of the sampling days and locations (Figure 2 and 3).

The relative abundance of sulfides trended similarly to the abundance of alcohols. Sulfide (S)-containing compounds are major contributors to the human decomposition VOC profile and were therefore expected to be present during most stages of decomposition.[21,22,24,25,30,41,50] The peak sulfide (and potentially nitrogen) sensor responses were recorded on day 7 during active decay (Figure 3). However, the peak in sulfide abundances recorded by GC×GC-TOFMS occured later, corresponding to the active decay stage of the torso (Figure 8, and Figure S2). It is likely that this pattern was observed as the volatilome collected by GC×GC-TOFMS represents the collective VOC profile from the entire body rather than being concentrated in smaller regions. In addition, as air flow could not disperse VOCs during this scenario, the relationship of surface area to VOC abundance is likely inverse to the sampling scenario of the NOS.E. For example, the sulfide compounds were likely diluted within the sampling container for the smaller head region. However, when the torso entered active decay, the increased surface area likely pre-concentrated the sulfide compounds within the sampling container. This may explain why sulfide detection differed between each sampling area for the NOS.E and the detection of the VOCs by GC×GC-TOFMS. Sulfide (S)-containing compounds were not present in large abundances in the mid to later stages of decomposition (active and advanced), which is supported by previous studies.[23,41]

Nitrogen (N)-containing compounds had a more defined trend in the GC×GC-TOFMS analysis, by which the relative abundance increased until day 7, before decreasing until they were no longer detected on day 60. Interestingly, this trend did not directly align with the NOS.E data for all sampling locations. The GC×GC-TOFMS nitrogen trend matched NOS.E responses for the head region, which had localized and advanced decomposition by which N- and S-containing compounds could be detected (Figure 2). N- and S-containing compounds were only detected by the NOS.E in a location away from the body (1 m away) on day 23 (Figure 4). The increased wind gust speed and change in wind direction were likely responsible for the detection of these compounds away from the body (Figures 4B and 4C). N- and S-containing compounds were detected both over the head and torso regions by the NOS.E in later stages of decomposition (day 68 and 76). It is likely that this sensor reaction can be attributed to S-containing compounds as N-containing compounds were not detected by the GC×GC-TOFMS (Figure 8).

Limitations

As this study used a single donor for the analysis, caution must therefore be taken when interpreting the results, particularly those related to the time since death. The donor was deposited on the surface of an Australian open eucalypt woodland. Not all missing persons will be located in an open outdoor

environment; therefore, this work would benefit from the inclusion of more human donors placed in different scenarios (e.g., surface-deposited, buried) to determine the utility of the NOS.E in different sampling conditions. Multiple replicates of NOS.E sampling to donors in different conditions will also allow for more accurate interpretation of detection results.

This study was able to determine that the current NOS.E prototype can be implemented to detect surface deposited human remains in an outdoor environment. As with detection dogs, the ability of the NOS.E to respond to human decomposition odour relies on its ability to detect the scent cone, which disperses based on temperature, wind direction, and wind speed.[51] In this work, the NOS.E was stationary and was not adjusted due to changing wind patterns. Despite this, the NOS.E was able to record responses related to human decomposition VOCs on most sampling days and from multiple sampling locations. Future work should be conducted where NOS.E samples are taken in context of changing wind direction to allow for more accurate detections of the scent cone. This more active sampling approach is likely to better capture the emitted volatiles and therefore improve the ability of the NOS.E to detect missing persons. Despite these limitations, this preliminary investigation into the field applicability of the NOS.E for the detection of surface deposited human remains shows great promise.

This work demonstrated a potential two-fold utility of the NOS.E. This first is for detecting decomposing human remains, while the second is the potential for its use in postmortem interval estimations from some regions. As sensor responses were recorded throughout many stages of decomposition, it is likely that the NOS.E has utility in detecting surface-deposited deceased individuals days and weeks after death.

STAR★METHODS

Detailed methods are provided in the online version of this paper and include the following:

- KEY RESOURCES TABLE
- RESOURCE AVAILABILITY
  - Lead contact
  - Materials availability
  - Data and code availability
- EXPERIMENTAL MODEL AND SUBJECT DETAILS
- METHOD DETAILS
  - Experimental site
  - Electronic nose sample collection
  - Sampling parameters
  - VOC sample collection
  - GC×GC-TOFMS analysis
- QUANTIFICATION AND STATISTICAL ANALYSIS

SUPPLEMENTAL INFORMATION

Supplemental information can be found online at https://doi.org/10.1016/j.isci.2023.106353.

ACKNOWLEDGMENTS

We are indebted to all the donors involved in research at AFTER and to the invaluable contribution they have made to forensic science. Ethics for this research was approved under the UTS Human Research Ethics Committee, Program Approval ETH18– 2999. The authors would also like to thank Sandali Alahakone for her help and support during sample collection. Funding: The Wildlife Crime Tech Challenge (WCTC), the United States Agency for International Development (USAID) (SS, MU). Australian Research Council, Discovery Early Career Research Award DE210100494 (MU).

AUTHOR CONTRIBUTIONS

Conceptualization: AB, DP, SS, MU; Methodology: AB, EL, AD, DP, TL, WZ; Investigation: AB, EL, AD, DP, TL, WZ; Visualization: AB, DP, MU; Supervision: MU, SS; Writing—original draft: AB, EL, AD, DP, MU; Writing—review & editing: AB, EL, AD, DP, TL, WZ, SS, MU.

DECLARATION OF INTERESTS

The authors declare that they have no competing interests.

INCLUSION AND DIVERSITY

We support inclusive, diverse, and equitable conduct of research.

Received: September 19, 2022
Revised: December 11, 2022
Accepted: March 3, 2023
Published: March 7, 2023

REFERENCES

1. Henderson, M., and Henderson, P. (1998). Missing People: Issues for the Australian Community (Australian Bureau of Criminal Intelligence Canberra).

2. Ward, J. (2018). The past, present and future state of missing persons investigations in Australia. Aust. J. Forensic Sci. *50*, 708–722.

3. Tidball-Binz, M. (2006). Forensic investigations into the missing. In Forensic Anthropology and Medicine (Springer), pp. 383–407.

4. Hughes, D.J. (1974). Homicide: Investigative Techniques (Thomas Springfield).

5. Haglund, W.D. (2001). Archaeology and forensic death investigations. Hist. Archaeol. *35*, 26–34.

6. O'Hara, G.L., and O'Hara, C.E. (2003). A Review Guide for Fundamentals of Criminal Investigation (Charles C. Thomas).

7. Pokines, J., Robinson, S., Mansz, J., Heidel, N., Jasny, K., Gilligan, J., Carmona, A., Kroll, J., Lavigne, S., and Calle, S. (2018). Success rate of forensic surface search for osseous remains in a New England, USA, environment. Forensic Anthropology *2*, 9–21.

8. Blau, S., and Sterenberg, J.F. (2016). Medicine, Anthropology: use of forensic archeology and anthropology in the search and recovery of buried evidence. Encyclopedia of Forensic and Legal Medicine, 236–245.

9. Corcoran, K.A., Mundorff, A.Z., White, D.A., and Emch, W.L. (2018). A novel application of terrestrial LIDAR to characterize elevation change at human grave surfaces in support of narrowing down possible unmarked grave locations. Forensic Sci. Int. *289*, 320–328.

10. Dutelle, A.W., and Becker, R.F. (2018). Criminal Investigation (Jones & Bartlett Learning).

11. DeGreeff, L.E., Weakley-Jones, B., and Furton, K.G. (2012). Creation of training aids for human remains detection canines utilizing a non-contact, dynamic airflow volatile concentration technique. Forensic Sci. Int. *217*, 32–38.

12. Parrott, E., Panter, H., Morrissey, J., and Bezombes, F. (2019). A low cost approach to disturbed soil detection using low altitude digital imagery from an unmanned aerial vehicle. Drones *3*, 50.

13. Watson, C.J., and Forbes, S.L. (2008). An investigation of the vegetation associated with grave sites in southern Ontario. J. Can. Soc. Forensic. Sci. *41*, 199–207.

14. Larson, D.O., Vass, A.A., and Wise, M. (2011). Advanced scientific methods and procedures in the forensic investigation of clandestine graves. J. Contemp. Crim. Justice *27*, 149–182.

15. Barone, P.M., and Di Maggio, R.M. (2019). Forensic geophysics: ground penetrating radar (GPR) techniques and missing persons investigations. Forensic Sci. Res. *4*, 337–340.

16. Pringle, J.K., Stimpson, I.G., Wisniewski, K.D., Heaton, V., Davenward, B., Mirosch, N., Spencer, F., and Jervis, J.R. (2020). Geophysical monitoring of simulated homicide burials for forensic investigations. Sci. Rep. *10*, 7544–7612.

17. Fischer, G. (1975). Symmetry properties of the surface impedance tensor for structures with a vertical plane of symmetry. Geophysics *40*, 1046–1050.

18. Daniels, D. (2004). In Ground Penetrating Radar, *Vol. 1*Ground Penetrating Radar (Iet).

19. Doolittle, J.A., and Bellantoni, N.F. (2010). The search for graves with ground-penetrating radar in Connecticut. J. Archaeol. Sci. *37*, 941–949.

20. Grip, W.M., Grip, R.W., and Morrison, R.D. (2000). Application of aerial photography and photogrammetry in environmental forensic investigations. Environ. Forensics *1*, 121–129.

21. Vass, A.A., Smith, R.R., Thompson, C.V., Burnett, M.N., Dulgerian, N., and Eckenrode, B.A. (2008). Odor analysis of decomposing buried human remains. J. Forensic Sci. *53*, 384–391.

22. Dekeirsschieter, J., Stefanuto, P.-H., Brasseur, C., Haubruge, E., and Focant, J.-F. (2012). Enhanced characterization of the smell of death by comprehensive two-dimensional gas chromatography-time-of-flight mass spectrometry (GCxGC-TOFMS). PLoS One *7*, e39005.

23. Forbes, S.L., and Perrault, K.A. (2014). Decomposition odour profiling in the air and soil surrounding vertebrate carrion. PLoS One *9*, e95107.

24. Vass, A.A., Smith, R.R., Thompson, C.V., Burnett, M.N., Wolf, D.A., Synstelien, J.A., Dulgerian, N., and Eckenrode, B.A. (2004). Decompositional odor analysis database. J. Forensic Sci. *49*, 760–769.

25. Statheropoulos, M., Spiliopoulou, C., and Agapiou, A. (2005). A study of volatile organic compounds evolved from the decaying human body. Forensic Sci. Int. *153*, 147–155.

26. Wong, J., and Robinson, C. (2004). Urban Search and Rescue Technology Needs: Identification of Needs*207771* (Federal Emergency Management Agency (FEMA) and the National Institute of Justice (NIJ). Document), p. 20.

27. Jones, K.E., Dashfield, K., Downend, A.B., and Otto, C.M. (2004). Search-and-rescue dogs: an overview for veterinarians. J. Am. Vet. Med. Assoc. *225*, 854–860.

28. Deo, A., Forbes, S.L., Stuart, B.H., and Ueland, M. (2020). Profiling the seasonal variability of decomposition odour from human remains in a temperate Australian environment. Aust. J. Forensic Sci. *52*, 654–664.

29. Ueland, M., Harris, S., and Forbes, S.L. (2021). Detecting volatile organic compounds to locate human remains in a simulated collapsed building. Forensic Sci. Int. *323*, 110781.

30. Clases, D., Ueland, M., Gonzalez de Vega, R., Doble, P., and Pröfrock, D. (2021). Quantitative speciation of volatile sulphur compounds from human cadavers by GC-ICP-MS. Talanta *221*, 121424.

31. Knobel, Z., Ueland, M., Nizio, K.D., Patel, D., and Forbes, S.L. (2019). A comparison of human and pig decomposition rates and odour profiles in an Australian environment. Aust. J. Forensic Sci. *51*, 557–572.

32. Statheropoulos, M., Agapiou, A., Spiliopoulou, C., Pallis, G.C., and Sianos, E. (2007). Environmental aspects of VOCs evolved in the early stages of human decomposition. Sci. Total Environ. *385*, 221–227.

33. Wilson, A.D., and Baietto, M. (2009). Applications and advances in electronic-nose technologies. Sensors *9*, 5099–5148.

34. Röck, F., Barsan, N., and Weimar, U. (2008). Electronic nose: current status and future trends. Chem. Rev. *108*, 705–725.

35. Ferrari, V., Marioli, D., Taroni, A., and Ranucci, E. (2000). Multisensor array of mass microbalances for chemical detection based on resonant piezo-layers of screen-printed PZT. Sensor. Actuator. B Chem. *68*, 81–87.

36. Tan, J., and Xu, J. (2020). Applications of electronic nose (e-nose) and electronic tongue (e-tongue) in food quality-related properties determination: a review. Artificial Intelligence in Agriculture *4*, 104–115.

37. Stejskal, S.M. (2012). Death, Decomposition, and Detector Dogs: From Science to Scene (CRC Press).

38. Zhang, W., Liu, T., Ueland, M., Forbes, S.L., Wang, R.X., and Su, S.W. (2020). Design of an efficient electronic nose system for odour analysis and assessment. Measurement *165*, 108089.

39. Stefanuto, P.-H., Perrault, K.A., Stadler, S., Pesesse, R., LeBlanc, H.N., Forbes, S.L., and Focant, J.-F. (2015). GC× GC–TOFMS and supervised multivariate approaches to study human cadaveric decomposition olfactive signatures. Anal. Bioanal. Chem. *407*, 4767–4778.

40. Payne, J.A. (1972). Insect succession and decompostition of pig carcasses in water. J. Ga. Entomol. Soc. *7*, 153–162.

41. Forbes, S.L., Perrault, K.A., Stefanuto, P.-H., Nizio, K.D., and Focant, J.-F. (2014). Comparison of the decomposition VOC profile during winter and summer in a moist, mid-latitude (Cfb) climate. PLoS One *9*, e113681.

42. Schotsmans, E.M.J., Van de Voorde, W., De Winne, J., and Wilson, A.S. (2011). The impact of shallow burial on differential decomposition to the body: a temperate case study. Forensic Sci. Int. *206*, e43–e48.

43. Perrault, K.A., Rai, T., Stuart, B.H., and Forbes, S.L. (2015). Seasonal comparison of carrion volatiles in decomposition soil using comprehensive two-dimensional gas chromatography–time of flight mass spectrometry. Anal. Methods *7*, 690–698.

44. Stadler, S., Stefanuto, P.-H., Brokl, M., Forbes, S.L., and Focant, J.-F. (2013). Characterization of volatile organic compounds from human analogue decomposition using thermal desorption coupled to comprehensive two-dimensional gas chromatography–time-of-flight mass spectrometry. Anal. Chem. *85*, 998–1005.

45. Perrault, K.A., Nizio, K.D., and Forbes, S.L. (2015). A comparison of one-dimensional and comprehensive two-dimensional gas chromatography for decomposition odour profiling using inter-year replicate field trials. Chromatographia *78*, 1057–1070.

46. Stadler, S., Desaulniers, J.-P., and Forbes, S.L. (2015). Inter-year repeatability study of volatile organic compounds from surface decomposition of human analogues. Int. J. Legal Med. *129*, 641–650.

47. Goff, M.L. (2009). Early Postmortem Changes and Stages of Decomposition, *Current Concepts in Forensic Entomology* (Springer), pp. 1–24.

48. Swann, L.M., Forbes, S.L., and Lewis, S.W. (2010). Analytical separations of mammalian decomposition products for forensic science: a review. Anal. Chim. Acta *682*, 9–22.

49. Dubois, L.M., Stefanuto, P.-H., Perrault, K.A., Delporte, G., Delvenne, P., and Focant, J.-F. (2019). Comprehensive approach for monitoring human tissue degradation. Chromatographia *82*, 857–871.

50. Cablk, M.E., Szelagowski, E.E., and Sagebiel, J.C. (2012). Characterization of the volatile organic compounds present in the headspace of decomposing animal remains, and compared with human remains. Forensic Sci. Int. *220*, 118–125.

51. Jezierski, T., Ensminger, J., and Papet, L. (2016). Canine Olfaction Science and Law: Advances in Forensic Science, Medicine, Conservation, and Environmental Remediation (CRC Press).

52. Troutman, L., Moffatt, C., and Simmons, T. (2014). A preliminary examination of differential decomposition patterns in mass graves. J. Forensic Sci. *59*, 621–626.

53. McKinney, W. (2010). Data structures for statistical computing in python. Proceedings of the 9th Python in Science Conference *445*, 51–56.

54. Harris, C.R., Millman, K.J., Van Der Walt, S.J., Gommers, R., Virtanen, P., Cournapeau, D., Wieser, E., Taylor, J., Berg, S., Smith, N.J., et al. (2020). Array programming with NumPy. Nature *585*, 357–362.

55. Virtanen, P., Gommers, R., Oliphant, T.E., Haberland, M., Reddy, T., Cournapeau, D., Burovski, E., Peterson, P., Weckesser, W., Bright, J., et al.; SciPy 1.0 Contributors (2020). SciPy 1.0: fundamental algorithms for scientific computing in Python. Nat. Methods *17*, 261–272.

56. Negri, L.H., and Vestri, C. (2017). Lucashn/Peakutils 1.

57. Pedregosa, F., Varoquaux, G., Gramfort, A., Michel, V., Thirion, B., Grisel, O., Blondel, M., Prettenhofer, P., Weiss, R., Dubourg, V., and Vanderplas, J. (2011). Scikit-learn: machine learning in Python. J. Mach. Learn. Res. *12*, 2825–2830.

58. Bedre, R. (2021). Reneshbedre/Bioinfokit: Bioinformatics Data Analysis and Visualization Toolkit.

59. Waskom, M. (2021). Seaborn: statistical data visualization. J. Open Source Softw. *6*, 3021.

60. Hunter, J.D. (2007). Matplotlib: a 2D graphics environment. Comput. Sci. Eng. *9*, 90–95.

STAR★METHODS

KEY RESOURCES TABLE

REAGENT or RESOURCE	SOURCE	IDENTIFIER
Chemicals		
Bromobenzene	Merck, Australia	CAS#: 108-86-1
Methanol	Merck, Australia	CAS#: 67-56-1
Helium 5.0	Coregas	UN#: 1046
Instruments		
NOS.E	Steven Su, Maiken Ueland	N/A
GC×GC-TOFMS	LECO Australia Pty Ltd.	N/A
Unity 2 Thermal Desorber	Markes International Ltd.	N/A
Series 2 ULTRA multi-tube autosampler	Markes International Ltd.	N/A
eVol® XR hand-held automated analytical syringe	SGE Analytical Science	N/A
Cold trap	Markes International Ltd	TenaxTA/Carbograph 1TD
Sorbent tubes	Markes International Ltd.	Carbograph 5TD and Tenax® TA
Primary column	Restek Corporation	Rxi®-624Sil MS
Secondary column	Restek Corporation	Stabilwax®
Software and algorithms		
ChromaTOF®	LECO Australia Pty Ltd.	version 4.51.6.0
Python	https://www.python.org/	3.7.6
Spyder	https://spyder-ide.org/	Spyder 4.0
Pandas	https://pandas.pydata.org/	1.2.4
NumPy	https://numpy.org/	1.20.1
SciPy	https://scipy.org/	1.6.2
Peakutils	https://peakutils.readthedocs.io/	1.3.3
scikit-learn	https://scikit-learn.org/	0.24.1
bioinfokit	https://github.com/reneshbedre/bioinfokit	2.0.8
seaborn	https://seaborn.pydata.org/	0.11.1
matplotlib	https://matplotlib.org/	3.3.4
Other		
Hobo U30 No Remote Communication data logger	OneTemp Pty Ltd	U30-NRC
Gas sensor 1	Figaro	TGS 2610 5U
Gas sensor 2	Figaro	TGS 2600
Gas sensor 3	Figaro	TGS 2612 5U
Gas sensor 4	Figaro	TGS 2603
Gas sensor 5	Figaro	TGS 2602
Aluminium Hood	Maiken Ueland	N/A

RESOURCE AVAILABILITY

Lead contact

If you have a request for more information or resources related to this paper, please contact Maiken Ueland (maiken.ueland@uts.edu.au).

Materials availability

No new materials were created during this study.

Data and code availability

- All data reported in this paper are available in the main text or the supplementary materials.
- This paper does not report original code.
- Any additional information required to reanalyze the data reported in this paper is available from the lead contact upon request

EXPERIMENTAL MODEL AND SUBJECT DETAILS

In order to determine the ability of the NOS.E, a recently deceased human donor in an outdoor environment was sampled and analysed at frequent intervals. This allowed the utility of the new technology to be tested during different decomposition stages (and therefore different times since death). This was done as missing persons may be missing for days to weeks. To further evaluate the NOS.E, the donor was also sampled using sorbent tubes and analysed via GC×GC-TOFMS, the commonly used benchtop method for VOC analysis.

A deceased female aged 75, weighing approximately 90 kg, with a height of 156 cm, was acquired through the University of Technology Sydney (UTS) Body Donation Program, with consent provided in accordance with the NSW Anatomy Act (1977). The research was approved under the UTS Human Research Ethics Committee Program Approval (UTS HREC REF NO. ETH18-2999). The cause of death for the donor was liver failure and metastatic cancer.

METHOD DETAILS

Experimental site

This research was conducted at the Australian Facility for Taphonomic Experimental Research (AFTER) located at the outskirts of Sydney New South Wales (NSW), Australia. A detailed description of the field site can be found in.[31]

The female donor was placed in a supine position, unclothed, at AFTER on a 5 × 5 m plot on 25/3/2020 (Day 0), which corresponds to the Australian autumn season. An anti-scavenging cage was placed over the remains when the donor was not being sampled. Visual observations of the decomposition state (i.e. photographs and written notes) were recorded once per sampling day. A Hobo Weather Station equipped with a Hobo U30 No Remote Communication data logger was used to monitor temperature (°C), humidity (%), wind speed (m/s) and gust (m/s), wind direction (°) and rainfall (mm) at an hourly rate and written to comma-separated value (.csv) files.

For complete transparency, it should be noted that the HOBO® weather station used to monitor the environment was located approximately 100 m away from the sampling site, and therefore gust speed experienced by the remains could differ slightly from the available readings. However, both the weather station and the remains were both located close to a fence line of the facility with a similar population of trees and shrubbery. It is therefore assumed that the gust speed readings are indicative of the environment experienced by the remains.

Electronic nose sample collection

For this study, the NOS.E[38] equipped with five metal oxide (MOX) gas sensors (Gas Sensors Australia, Mornington, VIC, Australia was used. (Table S1). This NOS.E and associated sensors was the only e-nose used for each sampling event and sample replicate. The sensor information was as follows: Sensor 1– Alcohols/Alkanes; Sensor 2 – Alcohols/Alkanes; Sensor 3 – Alkanes; Sensor 4 – Sulfur/Nitrogen; Sensor 5 – Nitrogen/Sulfur. These were selected and configured based on previous human decomposition studies[28,29,31] and an internal database (not published) and were quality checked for response against cadavers from the morgue at UTS in a controlled environment prior to the field study. This study was limited by commercially available VOC sensors for their use in the specific detection of human decomposition VOCs. For this work, the human decomposition volatilome database (housed internally at UTS) that comprises of VOCs produced by ~80 individuals at each decomposition stage were searched for most abundant chemical classes. Eight commercially available sensor types were purchased based on the

presence and relative abundance of these chemical classes to human decomposition volatilomes over each stage of decomposition. The NOS.E and each sensor were then trialled at the morgue, using a male donor. Each commercial sensor was trialled in two conditions. The first was for producing a response when presented to a human torso and the second was to the internal organs from the donor. Any sensor that could produce a response from either body part was then selected for further work (Figures S4 and S5).The sensors selected for this study were primarily target sensors for alcohol and alkanes along with nitrogen and sulfur-containing compounds.

NOS.E samples were taken from different areas above and away from the donor (Figure 9) to determine the influence of body region, distance and environmental factors on sensor responses. Five replicates were taken at each sampling location per day, with the exemption of day 20 and day 23. Here, samples were taken either of the torso and environment or from 1 m, 3 m, or environment due to electronic failure. The sensor replicate responses were averaged and the mean and standard deviations of each sensor response per sampling event can be found in Data S1 (Showing the mean and standard deviations of each individual sensor during each sampling event. Related to Figures 1, 2, 3, 4, 5, and 6).

Two regions of the body were chosen, since decomposition has been shown to vary within the same cadaver in a process referred to as differential decomposition.[52] The torso was selected, as it is predominantly where autolysis and putrefaction (i.e., the breakdown of bodily tissue) is observed.[52] The head was chosen due to its relative lack of fatty tissue and its quick skeletonisation process.[47] An environmental control sample was also sampled five times each sampling day for sensor response comparison. These samples were taken ~100m upwind from the donor and other surface deposited remains. The sampling time was selected after the responses for each sensor had reached a maximum value and remained constant for at least 10 s when sampling a human cadaver in the fresh stage of decomposition (where less volatiles are present). The longest active sampling time (80 s) was then employed for all sampling locations for standardisation. The sampling protocol involved a series of wash steps to eliminate any carryover or cross contamination and an active VOC sampling time of 80 s (table) for an overall baseline, sampling and cleaning duration of approximately 10 min. The baseline recovery time was selected based on when the NOS.E sensor responses returned to the original baseline values and remained constant for at least 30 s. The sensor responses that were acquired during the active VOC sampling duration were written to a text file (.txt) in a comma-separated format for each sample.

NOS.E sampling protocol

NOS.E operation	Time (s)
Chamber Wash I	200
Vacuum Time I	10
Baseline Setup	20
Vacuum Time II	10
Sample Time	80
Baseline Recovery	150
Chamber Wash II	150

The sampling parameters used during the NOS.E sample collection, including the wash and recovery times, used to clean and reset the instrument to prevent carry-over. In addition the baseline time is shown; this allows the instrument to equilibrate ensure there is no false reactivity to the environment.

Sampling parameters

Sampling occurred during the Australian Autumn season and continued into winter. The sampling frequency of the donor using the e-nose and the benchtop comparison (GC×GC-TOFMS) can be found in Table S2. Sampling occurred every other day initially before decreasing in due to the increased rate of the decomposition process during later stages. Sampling for both techniques were undertaken on the same day, unless unavailable, to which the closest day would be sampled.

VOC sample collection

VOC samples were collected from the headspace of the decomposing cadaver by placing an aluminum hood measuring 800 mm (H) x 1900 mm (L) x 1200 mm (W) over the donor. VOCs were allowed to accumulate for 15 min before being drawn into sorbent tubes (n = 3 per sampling event), packed with Carbograph 5TD and Tenax TA (Markes International Ltd., Llantrisant, UK), for 10 min at 100 mL/min using an ACTI-VOC™ low-flow sampling pump (Markes International Ltd., Australia). The sorbent tubes were attached to the sampling hood via a brass Swagelok fitting (Swagelok Company, Caringbah, Australia). Each tube was then wrapped in aluminum foil and transported to the laboratory for analysis in glass jars. Prior to sample analysis, each sorbent tube was injected with an internal standard of 0.2 μL of 10 ppm bromobenzene (CAS#: 108-86-1, HPLC grade, Sigma-Aldrich, Castle HIL, Australia) diluted in methanol (HPLC grade, Sigma-Aldrich, Australia) using an eVol XR hand-held automated analytical syringe (SGE Analytical Science, Sydney, Australia).

GC×GC-TOFMS analysis

A Markes Unity 2 Thermal Desorber and Series 2 ULTRA multi-tube autosampler (Markes International Ltd., Australia) were used to perform thermal desorption (TD) of the sorbent tubes as described in.[28,29,31] Briefly each tube was heated to 300°C for 4 min to allow for thermal desorption of compounds before being collected on a general-purpose cold trap (TenaxTA/Carbograph 1TD) at −10°C. The trap was desorbed at 300°C for 3 min with a split flow of 20 mL/min. Sample analysis was performed as described in[28,29,31] using a Pegasus 4D GC×GC-TOFMS (LECO, Castle Hill, NSW, Australia), that was connected to the TD unit using a 1 m uncoated fused-silica transfer line (Markes International Ltd.), heated to 120°C. The TD transfer line was joined to the primary column using an Ultimate Union kit (Agilent Technologies, Mulgrave, NSW, Australia). The GC×GC contains a Rxi-624Sil MS (30 m × 0.250 mm i.d., 1.40 μm film thickness) primary column and a Stabilwax (2 m × 0.250 mm i.d., 0.5 μm film thickness) secondary column (Restek Corporation, Sydney, NSW, Australia). A SilTiteTM μ-Union (SGE Analytical Science, Ringwood, VIC, Australia) was used to connect the primary and secondary columns. Helium was utilised as the carrier gas and was maintained at a constant flow rate of 1.0 mL/min. The oven temperature was set at 35°C and held for 5 min, then increased at a rate of 5 °C/min to 240°C. The temperature was then held here for 5 min. An offset of 15°C and 5°C were used for the secondary oven and modulator, respectively. Compounds were introduced onto the second column at a modulation period of 5 s with a 1 s hot pulse. The transfer line and ion source were held at 250°C and 200°C, respectively. The electron energy used for excitation was −70V. A total ion chromatogram (TIC) was collected for ions ranging from 29 to 450 amu at a rate of 100 spectra/s.

QUANTIFICATION AND STATISTICAL ANALYSIS

The environmental (.csv), NOS.E (.txt) and GC×GC-TOFMS (.xlsx) data files were processed using the Python programming language (Python 3.7.6, https://www.python.org/) in the Scientific Python Development Environment (Spyder 4.0, https://spyder-ide.org/). Data analysis was performed using pandas (1.2.4, https://pandas.pydata.org/),[53] NumPy (1.20.1, https://numpy.org/),[54] SciPy (1.6.2, https://scipy.org/),[55] peakutils (1.3.3, https://peakutils.readthedocs.io/),[56] scikit-learn (0.24.1, https://scikit-learn.org/),[57] and bioinfokit (2.0.8, https://github.com/reneshbedre/bioinfokit)[58] packages. Data visualization was performed using the seaborn (0.11.1, https://seaborn.pydata.org/)[59] and the matplotlib (3.3.4, https://matplotlib.org/)[60] packages.

For the environmental data, the daily averages for temperature, humidity, wind speed, gust speed and wind direction were calculated, while rainfall was given as the total for each day. The resulting data was graphed individually and also added to the sensor responses from the differing sampling regions.

To identify and process the NOS.E sensor responses, automated peak detection was performed on the sensor responses using the scipy and peakutils packages. Peak detection was performed using the scipy.find_peaks method with a prominence value set to 0.01. This method finds all local maxima in the data by simple comparison of neighboring values. When a local maximum is found, the left and right bases of the peak are determined and the prominence is calculated as the difference between the peak maximum and the lowest contour line (i.e. the higher of the two bases). It was chosen based on a manual assessment of the resulting peak hits to ensure that there were no false negative readings. The normalised responses of the detected peaks were determined by firstly estimating the baseline using the peakutils.baseline method with deg = 1 (i.e. a linear function) and then taking the difference between the response at the peak maxima and baseline response at the same reading. For sensors where the maximum sensor response was less than

5% of the minimum, or where there were no peaks using the peak detection algorithm at the given prominence value, the responses were given as an abundance of 0. The peak heights were then averaged across the five replicate samples (n = 5) taken each day and graphed. Principal component analysis (PCA) was performed on the averaged sensor readings for each stage of decomposition at each location using the PCA class from sckit-learn (https://scikit-learn.org/stable/modules/generated/sklearn.decomposition.PCA.html).[57] Firstly, the data for each component (i.e. sensor) is centered, but not scaled, followed by singular value decomposition (SVD) to two principal components.

The GC×GC-TOFMS data was also imported into python following the initial pre-processing: Data pre-processing was performed using ChromaTOF software (version 4.51.6.0, LECO, Australia). A similarity match of over 80% was required for tentative identification of the VOCs detected using the 2011 National Institute of Standards and Technology (NIST) mass spectral library database. The Statistical Compare feature of the software program was used for peak alignment across all samples. The samples were separated into control (n = 14) and experimental (n = 42) groups. VOCs were required to be present in 30% of the samples within a class or in two of the samples overall, due to the inherent differences expected between sampling days due to the decomposition process. The resulting list of VOCs was then imported into Microsoft Excel (version 16.42) where the internal standard, solvents and compounds derived from column bleed were manually removed. Compounds were subsequently categorised into compound classes based on their functional group(s). Once imported into python, the peak areas for each compound (analyte) identified by the GC×GC-TOFMS were averaged across the replicates for each day. An exclusion criterion was used; if the averaged peak area for experimental samples did not exceed 50% of the averaged peak area in the environmental control samples the analytes were removed. The remaining analytes were then summed according to their functional group and graphed.